6042 *Biochemistry* **2010,** *49,* 6042–6051
DOI: 10.1021/bi100303f

BIOCHEMISTRY
including biophysical chemistry & molecular biology
Article

Function of PsbO, the Photosystem II Manganese-Stabilizing Protein: Probing the Role of Aspartic Acid 157[†]

Johnna L. Roose,[‖] Charles F. Yocum,[‡,§] and Hana Popelkova*[,‡]

[‡]*Department of Molecular, Cellular, and Developmental Biology, and* [§]*Department of Chemistry, University of Michigan, Ann Arbor, Michigan 48109, and* [‖]*Department of Biological Sciences, Division of Biochemistry and Molecular Biology, Louisiana State University, Baton Rouge, Louisiana 70803*

Received March 1, 2010; Revised Manuscript Received June 17, 2010

ABSTRACT: The D157N, D157E, and D157K mutations in the *psbO* gene encoding the photosystem II (PSII) manganese-stabilizing protein from spinach, exhibit near-wild-type PSII binding but are significantly impaired in O_2 evolution activity and Cl^- retention by PSII [Popelkova et al. (2009) *Biochemistry 48*, 11920−11928]. To better characterize the role of PsbO-Asp157 in eukaryotic PSII, the effect of mutations in Asp157 on heat-induced changes in PsbO solution structure, O_2 release kinetics, and PSII redox reactions both within and outside the oxygen-evolving complex (OEC) have been examined. The data presented here show that Asn, Glu, or Lys mutations in PsbO-Asp157 modify PsbO thermostability in solution, which is consistent with the previously reported perturbation of the functional assembly of PsbO-Asp157 mutants into PSII that caused inefficient Cl^- retention by PSII. Fluorescence decay signals from PSII reconstituted with Asp157 mutants indicate that that the Q_A^- to Q_B transition on the PSII reducing side is unaffected, but complex alterations are detected on the PSII oxidizing side that affect the recombination of Q_A^- with the O_2-evolving complex. In addition, oxygen yield on the first flash is increased, which indicates an impaired ability of mutant-reconstituted PSII samples to decay back to the S_1 state in the dark.

Photosystem II (PSII)[1] in higher plants, algae, and cyanobacteria is a multisubunit redox enzyme that consists of intrinsic proteins, including the D1 and D2 proteins, CP43, CP47, and the α and *β* subunits of cytochrome b_{559}, along with several extrinsic polypeptides (PsbO, PsbQ, and PsbP in green algae and higher plants, PsbO, PsbU, and PsbV in cyanobacteria and red algae, as well as analogues of PsbP and PsbQ in cyanobacteria) (*1*, *2*). Water oxidation takes place at a site called the oxygen-evolving complex (OEC); extrinsic proteins facilitate retention of three inorganic cofactors (4 Mn, 1 Ca^{2+}, and 1 Cl^-) (*1*) and shield the Mn atoms from attack by endogenous reducing agents such as quinones (*3*). The OEC cycles through five distinct redox states, termed the S-states (S_n, where $n = 0-4$); the S_1 state is dark stable (*1*, *4*).

Maximal rates of O_2 evolution at physiological concentrations of the inorganic cofactors depend on the presence of the extrinsic proteins; PsbO, the manganese-stabilizing protein, plays a crucial role in stabilization of the Mn cluster and is required for high rates of O_2 evolution (*1*). Detailed characterization of the function of PsbO in PSII suggests a specific role for PsbO in Mn redox reactions. It has been shown that aspartate and/or glutamate residues of PsbO deprotonate during the S_1-S_2 transition (*5*) and that the structure of PsbO changes upon reduction of the Mn cluster with NH_2OH (*6*). Recent studies showed that PsbO functions to facilitate Cl^- retention by the OEC and that the protein stabilizes the Mn cluster in PSII by increasing the affinity of Cl^- for the OEC active site (*7*, *8*).

In solution, PsbO is a prolate ellipsoid (*9*, *10*) and behaves as a natively unfolded polypeptide (*11*) that exhibits features such as a low p*I* (5.2), a relatively high content of random coils and turns in its secondary structure, a high ratio of charged to hydrophobic residues, deviations in measurements of molecular mass, and thermostability (*12*−*14*). The latter property of PsbO was shown to be due to its ability to resist aggregation during heating (*15*). The natively unfolded structure of PsbO in solution may be an important feature for accommodation of the requirements for protein−protein interactions in the multisubunit PSII complex. Findings from previous studies indicate that PsbO binds in a two-step mechanism; docking of the protein at a PSII specific binding site is followed by folding/assembly of PsbO into PSII (*7*, *16*, *17*). Based on results obtained with the C15A and CC28,51AA PsbO mutants, this assembly process appears to consist of formation of the structural elements required for acceleration of O_2 evolution and induction of the separate structural features that stabilize O_2 evolution activity under prolonged illumination (*18*). This is consistent with the finding that PsbO gains some *β*-sheet elements at the expense of unordered coils and turns upon binding to PSII (*19*).

Binding and activity of PsbO in eukaryotic PSII have been studied in a number of site-directed mutants from spinach (*15*−*18*, *20*). Recent results reveal that mutagenesis of PsbO-Asp157 impedes O_2 evolution and Cl^- retention by PSII but not binding of PsbO to PSII. PsbO-Asp157 mutants were shown to be the first genetically modified

[†]This research was supported by a grant to H.P. and C.F.Y. from the National Science Foundation (MCB-0716541) and by grant to J.L.R. from the USDA National Institute of Food and Agriculture (National Research Initiative Competitive Grant 2008-35318-04605).

*Correspondence should be addressed to this author. Telephone: (734) 764-9543. Fax: (734) 647-0884. E-mail: popelka@umich.edu.

[1]Abbreviations: BSA, bovine serum albumin; CD, circular dichroism; Chl, chlorophyll; DCMU, 3-(3,4-dichlorophenyl)-1,1-dimethylurea; MES, 2-(*N*-morpholino)ethanesulfonic acid; MRE, mean residue ellipticity; OEC, oxygen-evolving complex; PS, photosystem; PsbO, the manganese-stabilizing protein; $Q_{A(B)}$, primary (secondary) quinone acceptor of PSII; SW-PSII, NaCl-washed photosystem II membranes depleted of 23 and 17 kDa extrinsic proteins; UW-PSII, urea and NaCl-washed photosystem II membranes depleted of PsbO, PsbP, and PsbQ (33, 23, and 17 kDa) extrinsic proteins; WT PsbO, recombinant wild-type PsbO.

 Published on Web 06/22/2010

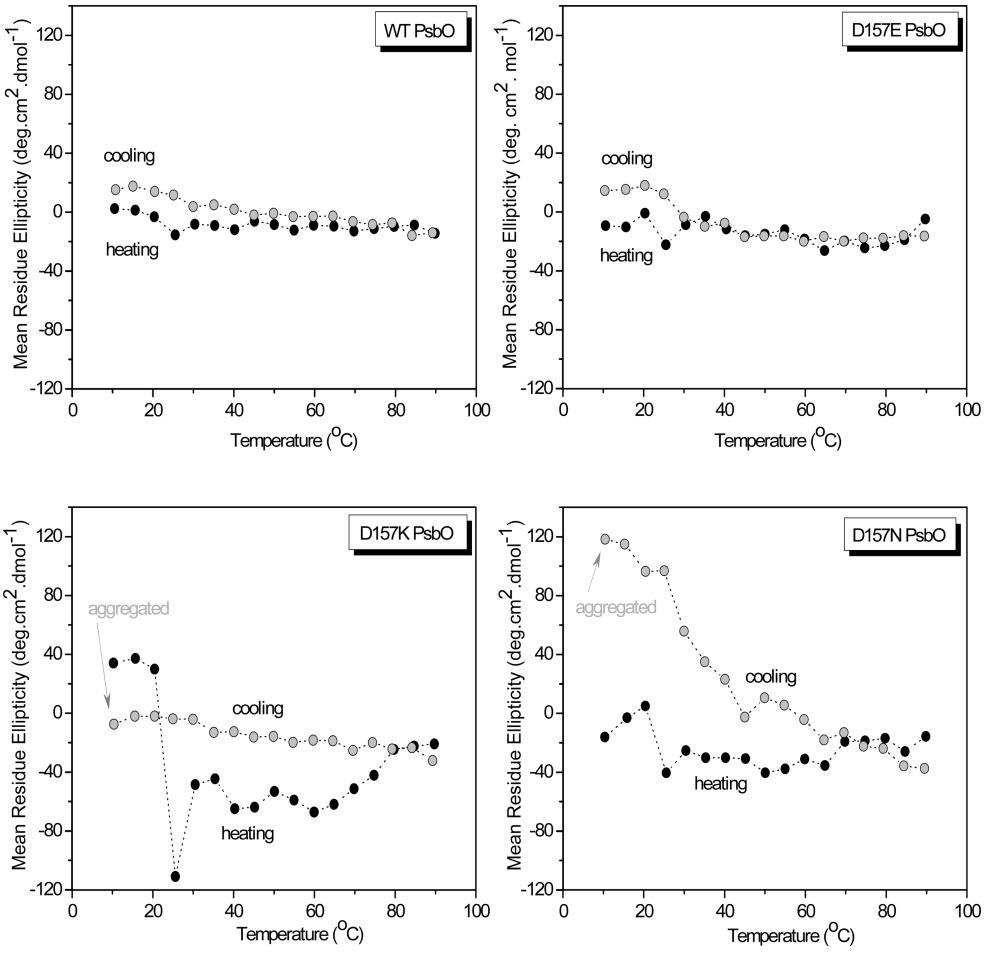

FIGURE 1: Temperature effects on the solution structure of WT, D157E, D157K, or D157N PsbO's monitored as mean residue ellipticity (MRE) at 291 nm (Trp signal) during heating (10 → 90 °C) and cooling (90 → 10 °C). PsbO's were dissolved in 10 mM KH_2PO_4 (pH 6). MRE was calculated on the basis of the protein concentration. Curves represent the average of two independent experiments. The experimental conditions were as follows: path length, 1 cm; sample volume, 1 mL; time constant, 3 s; bandwidth, 1 nm; temperature change, 3 °C/min; equilibration time, 2 min; dead band, 1 °C.

proteins from spinach with wild-type PSII binding that are significantly impaired in O_2 evolution activity. Since the solution structures of the D157N, D157E, and D157K mutants at 25 °C were found to be very similar to that of the wild-type protein, it was hypothesized that a defect in folding of the mutants during assembly into PSII might have lowered their ability to retain Cl^- in PSII (*21*).

To better characterize the deleterious effect of PsbO-Asp157 mutations on protein folding and stability that can affect a proper PSII assembly, we monitored the near-UV CD signal from the heated and cooled PsbO WT and Asp157 mutants in solution. To determine the specific defects in PSII function caused by the PsbO-Asp157 mutations, fluorescence decay after a single saturating flash and oxygen flash yield measurements were performed on membranes depleted of PsbO or reconstituted with various PsbO proteins. The results of these experiments show that replacement of PsbO-Asp157 by Asn, Glu, or Lys does not affect the kinetics of O_2 release during the $S_3-[S_4]-S_0$ transition or electron transfer between Q_A^- and Q_B. However, these mutations impair thermostability of PsbO in solution, affect recombination between Q_A^- and the oxidizing side of PSII, and enhance oxygen yield on the first flash.

MATERIALS AND METHODS

PsbO-Asp157 Mutants. The experiments presented here were carried out using the spinach PsbO mutants D157N, D157E, and D157K. The Asp mutations were prepared and characterized as described in ref *21*. Recombinant wild-type PsbO from spinach, that was characterized in a number of previous studies (*8*, *12*, *13*, *15*), was used as a control.

Reconstitution of PsbO-Depleted PSII with Recombinant PsbO. The UW-PSII membranes were prepared from spinach and stored as described (*7*, *13*). UW-PSII membranes were reconstituted with PsbO WT or Asp157 mutants (5−10 mol of PsbO/mol of PSII to ensure proper binding) for 1 h at room temperature in a reconstitution buffer containing 37 mM MES (pH 6), 100 μg/mL BSA, 0.3 M sucrose, 2% betaine (w/v), 10 mM Ca^{2+}, and 110 mM Cl^-. The Cl^- concentration used in these experiments is sufficient to saturate oxygen evolution activity; addition of higher concentrations of Cl^- fails to increase the activity of Asp157 mutants to control levels observed in PSII reconstituted with wild-type PsbO (*21*). The Chl concentration in the reconstitution mixtures was 200 μg/mL. The 1 mL aliquots of the reconstitution mixtures were centrifuged at 10000*g* and 4 °C for 10 min. Each pellet was resuspended in 65 μL of reconstitution buffer to obtain samples with Chl concentration of 3 mg/mL. The 15 μL aliquots of resuspended samples were stored at −70 °C.

Near-UV CD at Various Temperatures. Recombinant PsbO's were dialyzed in 10 mM KH_2PO_4 buffer (pH 6). The CD signal at 291 nm (assigned to Trp) during heating (10 → 90 °C) and cooling (90 → 10 °C) and near-UV CD spectra at 10, 25, and 90 °C were

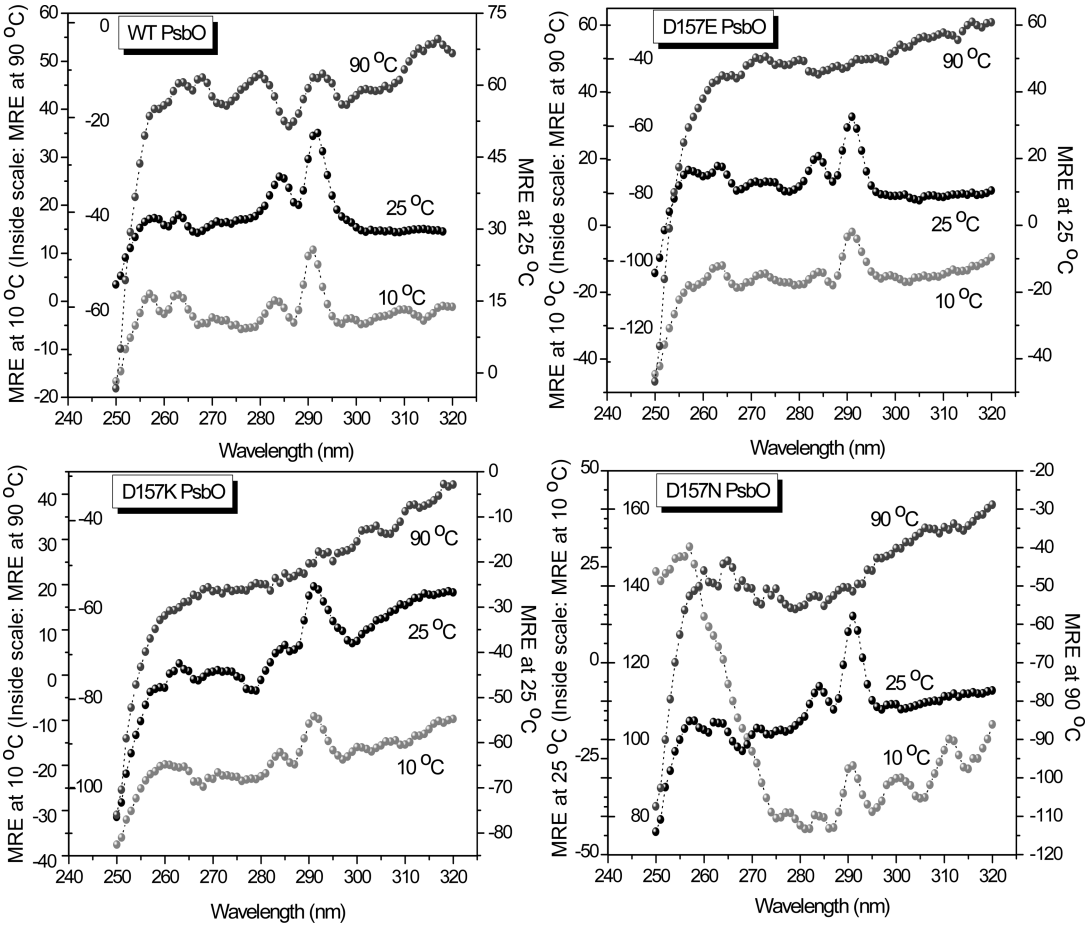

FIGURE 2: Effect of heating and cooling on the near-UV CD spectra of WT, D157E, D157K, or D157N PsbO's dissolved in 10 mM KH_2PO_4 (pH 6). Near-UV CD spectra were recorded at 25 °C before heating, at 90 °C, and at 10 °C after cooling. The spectrum in each panel has its own axis with inside or outside scales. The MRE was calculated on the basis of the protein concentration. Other experimental conditions are given in the legend to Figure 1.

measured using an AVIV 62 DS CD spectrometer to monitor heat-induced changes in the tertiary structure of recombinant PsbO's. The detailed experimental conditions are shown in the legend of Figure 1.

Fluorescence Experiments. Fluorescence decay after a single saturating flash was monitored with a Photon Systems Instruments (PSI) FL3000 dual modulation kinetic fluorometer (a commercial version of the instrument described in Nedbal et al. (*22*)). Both measuring and saturating flashes were provided by computer-controlled photodiode arrays. All samples were dark incubated for 5 min prior to measurement. Samples were assayed at a chlorophyll concentration of 10 μg/mL in reconstitution buffer. Similar results were also obtained with assay buffer (0.4 M sucrose, 50 mM MES−NaOH, pH 6.0, 10 mM $CaCl_2$, 80 mM NaCl). The fluorescence decay experiments monitored forward electron transfer from Q_A^- to Q_B in the absence of DCMU and charge recombination of Q_A^- with PSII donor-side components in the presence of DCMU (10 μM). The experimental data were analyzed using mathematical fitting that included three exponential decay components and one long-lived residual ($\tau > 10$ s) component (*23*). Data analysis was carried out using the Origin (version 6.1) program and software provided by Photon Systems Instruments. For each fluorescence trace, F_M was normalized on the fluorescence value measured at the time of the flash.

Oxygen Flash Yield Measurements. The oxygen flash yield measurements were performed on a bare platinum electrode (Artesian Scientific Co., Urbana, IL). PSII membranes samples containing 2.5−10 μg of chlorophyll in the same assay buffer mentioned above for the fluorescence experiments were applied to the bare platinum electrode, covered with an agarose disk (1% agarose in assay buffer), and dark incubated for 5 min. The electrode was polarized at 0.73 V for 20 s, and a series of 50 saturating flashes at 0.3 s intervals was supplied by an integrated, computer-controlled xenon flash lamp. S-state distributions and parameters were calculated by fitting using a four-state homogeneous model (*24*). The oxygen rise times were calculated by fitting peaks to the equation $f(t) = a + b(1 - e^{-k_r t}) + ce^{-k_d t}$ using the Origin 6.1 software package. The corresponding $t_{1/2}$ values for the rise and decay of the oxygen signals were calculated by $t_{1/2} = 0.693/k_r$ and $0.693/k_d$, respectively. Attempts were made to extend the dark incubation period to 20 min in experiments to probe the S_3 lifetime in reconstituted samples. Unfortunately, this treatment resulted in decreased signal intensities and artifacts (spikes) in the oxygen peaks (data not shown).

RESULTS

Heat-Induced Changes in the Solution Structure of WT PsbO and Asp157 Mutants. The solution structures of Asp157 mutants of PsbO at 25 °C are similar to that of wild-type PsbO (*21*). To probe these structures in greater detail under more extreme conditions, WT and PsbO's carrying a mutation in Asp157 were subjected to heating from 10 to 90 °C, followed by cooling from 90 to 10 °C. Figure 1 shows the effect of this treatment on the tertiary structure of all four PsbO proteins in

solution, monitored by mean residue ellipticity (MRE) at 291 nm, a signal that originates from Trp241 in a hydrophobic environment (*12*, *25*). As can be seen, WT PsbO exhibited a gradual and continuous change during heating, recorded as a decrease in MRE (Figure 1, upper left panel). The melting curve did not show a clear transition point. A significant drop in MRE between 10 and 25 °C (Figure 1) was found to be a reproducible instrument artifact, because this decrease was not observed when the CD signal for the wild-type protein was measured in the spectral mode of the CD spectrometer at 10 and 25 °C (data not shown). In Figure 2, the upper left panel presents the near-UV CD spectra for WT PsbO at 25 °C (before heat treatment), 90 °C (during heating), and 10 °C (after cooling). Well-defined near-UV CD peaks correspond to Trp (291−293 nm), Tyr (285−287 nm), and Phe (258−264 nm) (*16*, *25*). The WT PsbO protein appears to retain some elements of its tertiary structure during heating, because the near-UV CD spectrum of WT PsbO at 90 °C exhibits the well-defined, albeit modified, peaks observed at 25 °C. This finding differs somewhat from what was observed for the secondary structure of wild-type PsbO; this structure is lost upon heating, and its melting curve exhibits the clear transition point of 61 or 65 °C in the native and recombinant proteins, respectively (*12*). The nearly identical wild-type spectra recorded before (25 °C) and after (10 °C) heat treatment demonstrate that WT PsbO is thermostable, owing to its ability to regain its original tertiary solution structure upon cooling. The cooling curve for recombinant wild type in Figure 1, upper left panel, shows that the reappearance of WT PsbO tertiary structure occurs by a continuous mechanism. In contrast to WT PsbO, the Asp157 mutants did not exhibit a continuous decline in MRE upon heating. A decrease in MRE shifted to a gradual increase as heat treatment reached a temperature of 50 or 60 °C (Figure 1, upper right and both lower panels). Moreover, the reproducible instrument artifact described above for WT PsbO is more apparent in the Asp157 mutants, especially in the D157K sample (Figure 1). As compared to recombinant wild-type PsbO, the absence of well-defined peaks in the near-UV CD spectra of Asp157 mutants at 90 °C indicates that the mutants fail to preserve residual tertiary structure at 90 °C (Figure 2). A modification of the CD spectra recorded at 10 °C after cooling, compared to the spectra obtained at 25 °C before heat treatment, suggests that the environment of aromatic amino acids in the PsbO mutants has changed after undergoing the heating−cooling cycle (Figure 2, upper right and both lower panels). Furthermore, the apparent loss of thermostability of the D157K and D157N proteins was reflected in a significant loss of ability to resist aggregation; D157K formed large clotted aggregates in the potassium buffer, while the D157N solution became cloudy after cooling.

Fluorescence Decay Kinetics for WT PsbO and Asp157 Mutants. The Q_A^- reoxidation kinetics detected after a single turnover flash in either the presence or the absence of DCMU were used to probe electron transfer kinetics in UW-PSII preparations and in samples reconstituted with WT PsbO and Asp157 mutants. When measured in the absence of DCMU, the fluorescence decay reflects forward electron transfer from Q_A^- to Q_B and can detect alterations in electron transfer reactions on the reducing side of PSII. In the presence of DCMU, forward electron transfer is blocked, and the fluorescence decay represents charge recombination with S-states or $Y_Z^\bullet$ on the oxidizing side of PSII.

The fluorescence decays after a single flash in the absence of DCMU for UW-PSII and UW-PSII reconstituted with PsbO WT or Asp157 mutants are shown in Figure 3, and the corresponding kinetic parameters are presented in Table 1. The decay curves have been fit to three exponential components (*23*). Each component is characterized by two kinetic parameters, a time constant and an amplitude that represent the kinetics and the magnitude, respectively, of the particular process that contributes to the overall fluorescence decay. The fast component reflects electron transfer from Q_A^- to Q_B (*26*, *27*), while the middle exponential decay can be ascribed to electron transfer from Q_A^- to Q_B in PSII reaction centers where plastoquinone has to bind to the Q_B site before the electron is transferred from Q_A^- (*28*). There are ~2.5 plastoquinones per PSII in intact PSII membranes (see ref *29*). The slow decay component is associated with charge recombination between Q_A^- and PSII donor-side components (*30*), and the residual fraction may be related to the equilibrium between Q_A^- and Q_B (*31*). Figure 3 and Table 1 show that PsbO depletion does not drastically affect the fast and middle exponential decays, although some reducing side defects exist (see ref *29* for further discussion). The major differences between the UW-PSII and WT PsbO-reconstituted samples can be seen in the slow and residual components which reflect charge recombination with donor-side components. The absence of the PsbO protein retards the slow component (17 s, 31% vs 2.9 s, 27%) and increases the residual fraction (8% vs 3.4%) relative to the sample reconstituted with WT PsbO. The effect of Asp157 mutagenesis in PsbO on the fast and intermediate exponential decays and on an amplitude for the slow component is negligible,

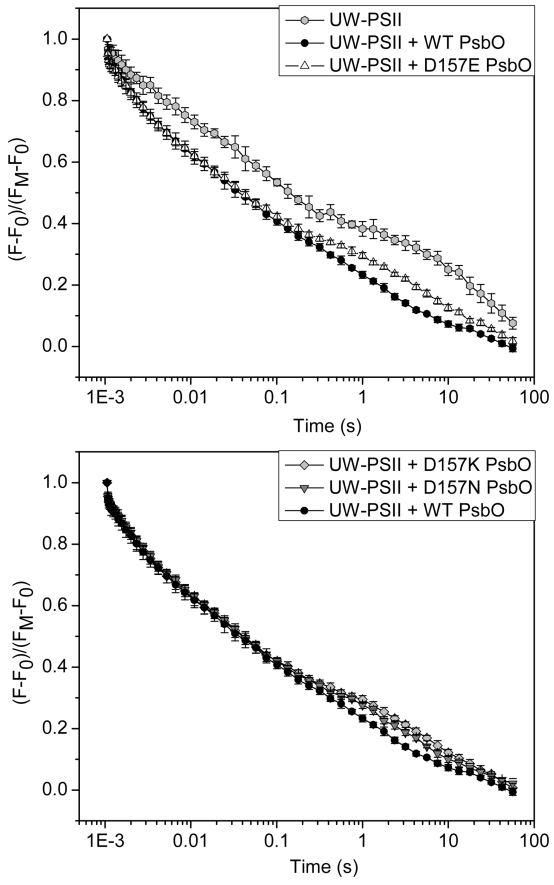

FIGURE 3: Q_A^- reoxidation kinetics in the absence of DCMU after a single saturating flash applied to UW-PSII and to PSII reconstituted with WT PsbO or the Asp157 mutants. The sample reconstituted with WT PsbO is shown in each panel for purposes of comparison. Data were collected after dark incubation for 5 min. Points are the averages, and vertical bars at each point give the standard deviation; $n = 6-9$.

Table 1: Kinetic Parameters of Q_A^- Reoxidation in the Absence of DCMU after a Single Saturating Flash Applied to UW-PSII and PSII Reconstituted with WT PsbO or D157N, D157E, or D157K PsbO Mutants[a]

	fast phase		intermediate phase		slow phase		
sample	t_1 (ms)	% amplitude	t_2 (ms)	% amplitude	t_3 (s)	% amplitude	% residual amplitude
UW-PSII	3.0 ± 1	29 ± 1	110 ± 20	32 ± 2	17 ± 2.0	31 ± 2	8 ± 3
UW-PSII + WT PsbO	2.0 ± 1	42 ± 5	60 ± 10	29 ± 3	2.9 ± 0.4	27 ± 2	3.4 ± 0.4
UW-PSII + D157E PsbO	2.1 ± 0.2	41 ± 1	63 ± 8	28 ± 0.9	6.0 ± 0.5	27 ± 0.6	4.7 ± 0.8
UW-PSII + D157K PsbO	2.2 ± 0.4	42 ± 2	60 ± 10	28 ± 1	6.4 ± 0.7	27 ± 1	3.8 ± 0.9
UW-PSII + D157N PsbO	2.2 ± 0.2	40 ± 1	61 ± 2	29 ± 1	4.3 ± 0.2	26 ± 0.9	4.6 ± 0.9

[a] n = 6-9; error = 1.0 standard deviation.

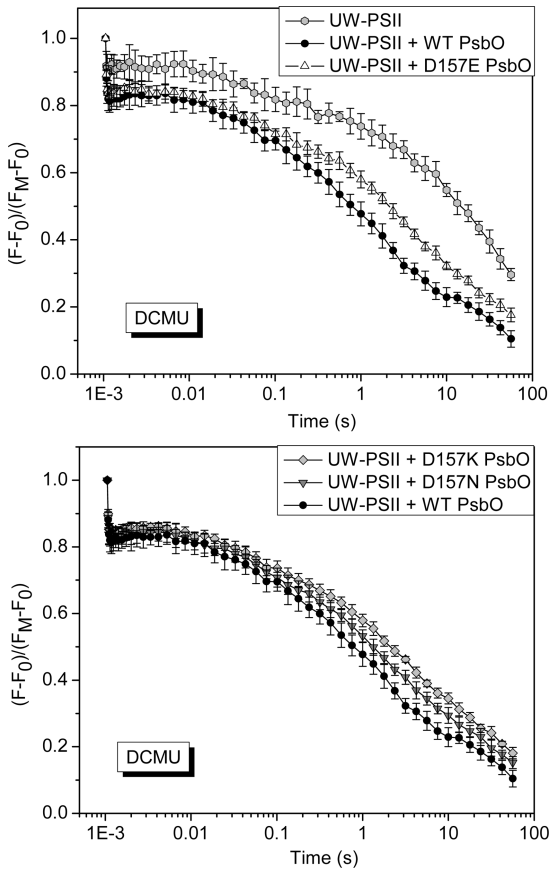

FIGURE 4: Q_A^- reoxidation kinetics in the presence of DCMU (10 μM) after a single saturating flash applied to UW-PSII and to PSII reconstituted with WT PsbO or the Asp157 mutants. The sample reconstituted with WT PsbO is shown in each panel as the control for purposes of comparison. Data were collected after dark incubation for 5 min. Points are the averages, and vertical bars at each point give the standard deviation; n = 6−9.

but the time constants for the slow phase (6, 6.4, 4.3 s) as well as the residual amplitudes (4.7%, 3.8%, 4.6%) are slightly increased in UW-PSII reconstituted with PsbO-Asp157 mutants as compared to UW-PSII reconstituted with WT PsbO. Although it has been shown that removal of extrinsic PsbP and PsbQ subunits from the oxidizing side of PSII can affect the reducing side of the system (*29*), the results in Figure 3 and Table 1 indicate that mutagenesis of PsbO-Asp157 and the defects created by these mutations do not alter electron transfer on the reducing side; on the contrary, both the absence of PsbO and mutagenesis of PsbO-Asp157 alter reaction kinetics at the PSII oxidizing side.

Figure 4 presents the fluorescence decay kinetics monitored in the presence of DCMU, where electron transfer from Q_A^- to Q_B is blocked, in order to elucidate the effect of the PsbO−D157 mutation on the kinetics of charge recombination between Q_A^- and the oxidizing side of PSII. The fluorescence decay curves in Figure 4 can be separated into three exponential components (*23*). In this case, the fast component represents the fraction of PSII centers which lack a functional Mn cluster and Q_A^- transfers electrons to $Y_Z^\bullet$ (*32*). The slow phase is associated with charge recombination between Q_A^- and the S_2 state (and possibly the S_3 state) (*33*). The origin of the intermediate component is less clear, but it has been reported to be related to faster charge recombination between Q_A^- and the S_2 state or perhaps an altered S_2 state (*23*). Finally, the residual component represents very slow charge recombination between Q_A^- and the oxidizing side of PSII. The kinetic parameters corresponding to Figure 4 are presented in Table 2. Figure 4 and Table 2 show that the time constant of the fast component (about 60 ms) is similar for all samples analyzed; however, the amplitude of the fast component in PsbO-depleted PSII (13%) is slightly smaller relative to the reconstituted samples (17−19%). The origin of this small difference is unclear, but one explanation might be that PsbO rebinding to PSII creates a structure in which a fraction of PSII centers retains Mn that is nonfunctional and which escapes detection in PsbO-depleted PSII membranes. Alternatively, the process of reconstitution of PsbO to PSII might create a small population of defective centers without a functional Mn cluster, which are detected in the reconstituted samples. In any case, this small population of nonfunctional PSII centers does not contribute to steady-state oxygen evolution activity and thus cannot be the cause of the low activity detected in samples reconstituted with PsbO-Asp157 mutants. The increased values observed for the slow and residual components for the UW-PSII sample (38 s, 51%, and 21%, respectively) compared to the sample containing WT PsbO (22 s, 27%, and 12%) highlight the defect on the PSII oxidizing side (the more stable S_2 state) in the absence of PsbO. The Asp157 mutants have slow component time constants similar to those of the wild-type protein, but the corresponding amplitudes are somewhat higher (31−33% vs 27%) than those observed for WT PsbO. Likewise, the residual components for the Asp157 mutants are higher relative to wild type (17−19% vs 12%). Taken together, these higher amplitudes may indicate altered recombination processes between Q_A^- and the oxidizing side of PSII reconstituted with PsbO-Asp157 mutants, as compared to PSII reconstituted with WT PsbO. Since the slow component time constants are similar among the samples, it is not possible to attribute these increases in the slow and residual amplitudes as being due simply to an increase in stability of the S_2 state (*33*). The contribution of these parameters to the curves observed in Figure 4 results in the small, but significant deviation of the traces of samples reconstituted with Asp157 mutants from

Table 2: Kinetic Parameters of Q_A^- Reoxidation after a Single Saturating Flash Applied to DCMU-Treated UW-PSII and PSII Reconstituted with WT PsbO or D157N, D157E, or D157K PsbO Mutants[a]

	fast phase		intermediate phase		slow phase		
sample	t_1 (ms)	% amplitude	t_2 (s)	% amplitude	t_3 (s)	% amplitude	% residual amplitude
UW-PSII	60 ± 20	13 ± 2	3.0 ± 2.0	16 ± 3	38 ± 16	51 ± 6	21 ± 9
UW-PSII + WT PsbO	60 ± 20	19 ± 3	1.2 ± 0.3	42 ± 3	22 ± 8	27 ± 2	12 ± 3
UW-PSII + D157E PsbO	58 ± 14	18 ± 2	2.0 ± 0.5	32 ± 4	22 ± 7	32 ± 4	19 ± 3
UW-PSII + D157K PsbO	56 ± 9	17 ± 2	1.7 ± 0.4	32 ± 5	25 ± 8	33 ± 2	18 ± 4
UW-PSII+D157N PsbO	50 ± 10	18 ± 1	1.4 ± 0.3	34 ± 4	20 ± 7	31 ± 3	17 ± 3

[a] n = 6-9; error = 1.0 standard deviation.

that of wild type beyond 100 ms, whose origin, as noted above, cannot be determined.

Oxygen Flash Yield Experiments. Short saturating light pulses can be used to advance PSII centers stepwise through the five S-states (S_0−S_4). The oxygen yield patterns produced by a series of these flashes provide detailed information on the turnover of the OEC. Typically, the dark incubation period prior to the measurement forms the PSII centers that decay back to the S_1 state and results in a maximal peak after the third flash. Figure 5 shows a typical oxygen flash yield pattern observed for UW-PSII and UW-PSII reconstituted with either WT or Asp157 mutants of PsbO. In the presence of WT PsbO, PSII membranes display a typical oxygen flash yield pattern with a maximal peak after the third flash. The oxygen flash yield pattern of PsbO-depleted PSII membranes is qualitatively very different, with the largest oxygen yield after the first flash. The oxygen flash yield pattern observed for D157E partially restores the pattern observed with WT PsbO, but this mutant exhibited a higher oxygen yield on the first flash relative to the wild-type sample (Figure 5). The oxygen flash yield patterns observed for D157K and D157N were almost identical to that observed for D157E (data not shown). It should be emphasized that oxygen flash yield patterns shown here originate from signals with different absolute values. The UW-PSII sample exhibited a very low absolute signal; 10 μg of Chl was needed per measurement to obtain the maximal peak value of 1.5−2.5 mV. Among the PsbO-reconstituted samples, where 5 μg of Chl was used in each sample per measurement, WT had the highest absolute signal intensity (1.3−2 mV); PSII samples reconstituted with PsbO mutants exhibited maximum peak values in a similar range (0.4−1 mV for D157E, 0.9−1.5 mV for D157K, and 0.7−1.5 mV for D157N). The oxygen yield on the first flash after normalization of all data to the height of the third flash is shown in Figure 6. Samples reconstituted with PsbO-Asp157 mutants and PsbO-depleted samples exhibit about 15-fold and 150-fold higher oxygen yield on the first flash than do samples reconstituted with WT PsbO. To exclude the possibility that the high oxygen yield on the first flash comes from an interaction of the Mn cluster with hydrogen peroxide (*34*), oxygen flash yield was also measured in the presence of catalase (data not shown); the result was the same as that in the absence of catalase (Figure 6). Additional control experiments were carried out using EDTA or Mn^{2+}; addition of EDTA or Mn^{2+} to samples had no effect on oxygen yield on the first flash (Figure 6) (data not shown). These results indicate that the unusual oxygen yield on the first flash does not arise from reactions between electrode-generated peroxide and adventitious Mn^{2+} (*34*); instead, it originates from PSII centers that do not decay back to the S_1 state in the dark but remain in the S_3 state.

Table 3 presents the S-state parameters and S-state distribution prior to the first and second flashes, calculated for UW-PSII and UW-PSII reconstituted with PsbO WT or Asp157 mutants. Quantitative analysis revealed that mutations in Asp157 have no

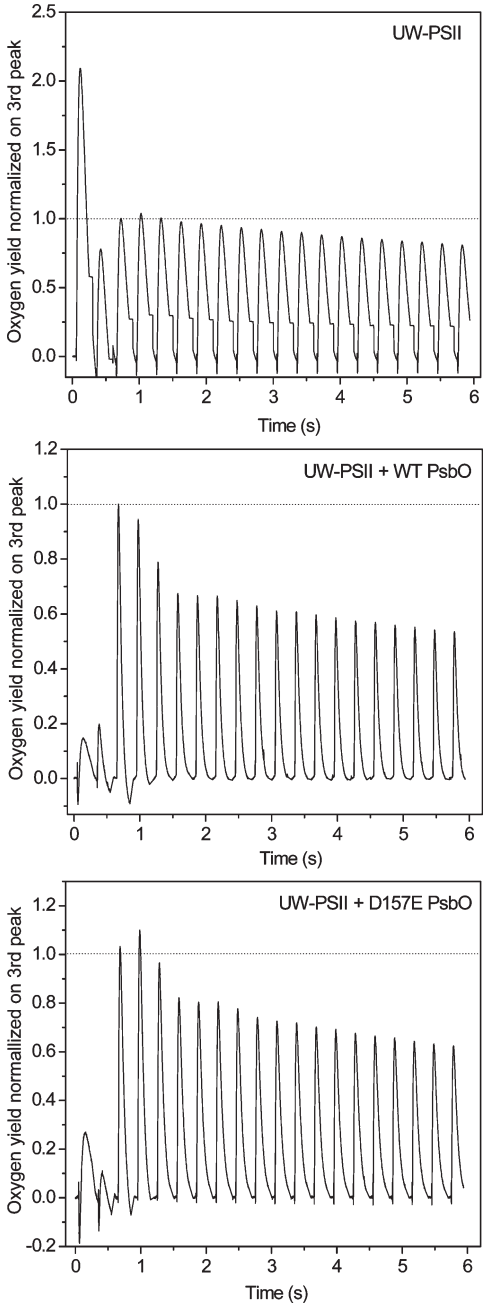

FIGURE 5: Data illustrating the typical oxygen flash yield patterns obtained from UW-PSII and PSII reconstituted with WT or D157E PsbO. Curves were normalized to the height of the third peak (oxygen yield after the third saturating flash).

effect on misses, single hits, double hits, or deactivations, while PsbO extraction increases the probability for double hits and decreases the probability of misses. The S-state distribution prior to the first and second flashes is reflected in the results in Figures 5 and 6; most notably, the four-state homogeneous model used to fit the data generally fails to compute the S-state distributions prior to the first flash for these samples, resulting in negative percentages with large error values for some of the S-states. However, this statistical model could be used to determine the S-state distribution prior to the second flash for all samples. Analysis of this set of data reveals that in the presence of WT PsbO the majority of PSII centers are distributed between the S_1 and S_2 states prior to the second flash, which is consistent with the fact that most of these centers decayed back to the S_0 and S_1 states during the initial dark-incubation period. In contrast, in the absence of PsbO, the population of PSII centers in the different S-states is distributed more evenly, resulting in much larger populations of PSII reaction centers in the S_0 and S_3 states compared to those observed in the presence of WT PsbO (Table 3). An increased dark stability of the S_2 and S_3 states in the absence of the PsbO protein can explain these results (*35*). The S-state distributions of samples reconstituted with Asp157 mutants largely resemble those of the wild-type sample with the majority of PSII centers distributed between the S_1 and S_2 states. However, the PsbO mutants display an increase in the population of PSII centers in S_0. Because the kinetic parameters are similar among the reconstituted samples, this result can be explained by an increase in the dark stability of the S_3 state in samples reconstituted with PsbO-Asp157 mutants.

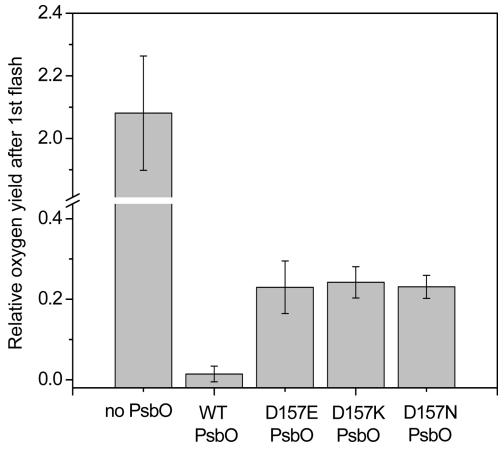

FIGURE 6: The oxygen flash yield after the first saturating flash relative to the oxygen yield after the third saturating flash. Flashes were applied to PsbO-depleted PSII and samples reconstituted with WT PsbO or Asp157 mutants. Data were normalized from the baseline to the height of the third peak (oxygen yield after the third saturating flash). Columns are the averages and vertical bars on each column represent the standard deviation; $n = 8-15$.

Analysis of the rise time of the oxygen peaks provides an estimate of the oxygen release during the $S_3-[S_4]-S_0$ transition. Peaks corresponding to signals after 30−40 flashes by which time the S-states were randomly distributed were compared (Table 4). The O_2 release time for a PsbO-depleted sample was ~37 ms. Reconstitution of UW-PSII with either WT or an Asp157 mutant of PsbO shortened O_2 release time to an interval between ~10 and ~13 ms, indicating that mutagenesis in PsbO-D157, in contrast to PsbO depletion, did not affect −O−O− bond formation.

Table 4: Oxygen Release Kinetic Parameters for PsbO-Depleted PSII Membranes and Samples Reconstituted with WT PsbO or D157N, D157E, or D157K PsbO Mutants[a]

sample	rise $t_{1/2}$ (ms)
UW-PSII	37 ± 4
UW-PSII + WT PsbO	11 ± 1
UW-PSII + D157E PsbO	13 ± 1
UW-PSII + D157K PsbO	12 ± 1
UW-PSII + D157N PsbO	10 ± 1

[a] $n = 20-24$; error, ±1.0 standard deviation.

Table 3: S-State Parameters and Distributions for UW-PSII and PSII Reconstituted with WT PsbO, D157E PsbO, D157K PsbO, or D157N PsbO[a]

	no PsbO	WT PsbO	D157E PsbO	D157K PsbO	D157N PsbO
			S-State Parameter		
misses	13.5 ± 4.6	24.0 ± 4.4	22.5 ± 5.1	23.6 ± 4.8	23.3 ± 2.3
single hits	51.0 ± 2.8	56.0 ± 5.8	58.6 ± 5.1	59.0 ± 3.1	59.2 ± 1.8
double hits	24.1 ± 4.2	9.2 ± 5.1	5.1 ± 3.8	3.5 ± 1.2	5.5 ± 1.4
deactivations	10.0 ± 3.9	7.7 ± 2.8	10.9 ± 4.0	11.0 ± 2.7	9.1 ± 0.7
			S-State Distributions Prior to First Flash		
S_0	−6.9 ± 16.2	26.9 ± 19.6	45.0 ± 10.1	37.6 ± 13.4	40.0 ± 8.7
S_1	37.9 ± 24.8	94.6 ± 39.0	67.7 ± 14.6	63.8 ± 12.0	67.3 ± 6.7
S_2	−1.8 ± 20.0	−27.6 ± 29.2	−21.4 ± 10.6	−8.7 ± 3.0	−15.7 ± 5.4
S_3	71.9 ± 11.4	6.0 ± 8.0	8.9 ± 4.6	7.3 ± 1.3	8.4 ± 1.5
			S-State Distributions Prior to Second Flash		
S_0	37.1 ± 3.3	12.0 ± 5.5	20.8 ± 1.4	19.6 ± 1.9	19.9 ± 1.5
S_1	20.4 ± 4.1	40.7 ± 5.7	42.3 ± 2.1	38.5 ± 2.7	39.7 ± 2.5
S_2	26.3 ± 3.6	47.2 ± 4.5	37.8 ± 3.2	38.5 ± 4.7	40.4 ± 2.8
S_3	16.2 ± 1.9	0.1 ± 3.5	−0.9 ± 2.6	3.4 ± 1.0	0.0 ± 1.8

[a] $n = 8-15$; error, ±1.0 standard deviation.

DISCUSSION

Asp157 Mutations Impair Thermostability of PsbO in Solution and Functional Assembly of PsbO into PSII. The PsbO-Asp157 mutants characterized here exhibit high-affinity binding of two copies of the protein per PSII reaction center, but they restore only ~40% of the activity of recombinant wild type (~30% of SW-PSII control) and cannot efficiently retain Cl^- in PSII (*21*). Solution structures of D157N, D157E, and D157K PsbO at 25 °C were found to be similar to that of WT PsbO (*21*). The detailed structural analysis presented here shows, however, that the solution structure of the Asp157 mutants behaves somewhat differently from that of WT when the PsbO proteins are heated and then cooled in 10 mM KH_2PO_4 buffer (pH 6). Under these conditions, retention of some elements of tertiary structure (monitored by the MRE of Trp241) at 90 °C and full recovery of PsbO tertiary solution structure upon cooling to 10 °C are observed only for the recombinant wild-type protein; all of the PsbO-Asp157 mutants exhibit complete loss of their tertiary structures during heating (90 °C) and incomplete recovery of tertiary structure after cooling (10 °C) (Figures 1 and 2). This result suggests that the loss of thermostability by Asp157 mutants is probably due to a perturbation of a very specific interaction that normally occurs in WT between D157 and the PsbO backbone. Heating revealed that the loss of this interaction due to a mutation in PsbO-D157 likely generates a structural disruption that cannot be recovered by substitution of Lys, Asn, or Glu. As a result, these mutated proteins display similar properties and exhibit similar impaired interactions with PSII. It has been shown previously that the PsbO secondary structure undergoes additional folding, to form β-sheet, after docking at a PSII binding site and that this process is important for functional assembly of the PsbO protein into PSII (*7*, *16*, *18*−*20*). Both a loss of thermostability of PsbO in solution (Figures 1 and 2) and inefficient Cl^- retention by PSII (*21*) due to mutations of Asp157 would indicate that functional folding and assembly of PsbO into PSII require Asp157. This negatively charged residue might form a salt bridge with Arg161, which affects functional assembly and efficient Cl^- retention by PSII (*7*). D157 is a part of the large flexible loop of PsbO (*21*), and it could be argued that greater conformational flexibility of this loop should help the protein to accommodate a mutation, especially the Asp → Glu mutation. Data obtained with the D48G and R51Q mutants of native thermostable and molten globule variants of chorismate mutase (CM) were interpreted to indicate the opposite; the higher rigidity of the natural variant of CM can more easily reinforce positioning of the backbone. As electrostatic interactions require precise positioning of the residues involved in these interactions, a high degree of conformational mobility of the molten globule variant of CM imposes an energetic cost for maintenance of the functional conformation of the protein backbone (*36*).

Mutagenesis of PsbO-D157 Affects Oxidizing-Side Reactions of PSII but Has No Effect on Kinetics of O_2 Release, S-State Parameters, and Electron Transfer from Q_A^- to Q_B. Previous experiments with Asp157 mutants showed that although rebinding to PSII occurs with an affinity and stoichiometry similar to that of the wild-type protein, Cl^- retention by PSII reconstituted with Asp157 mutants is impaired, as evidenced by an increase in the Cl^- K_M; additions of excess Cl^- in amounts that would normally be sufficient to permit formation of the S_2 and S_3 states (*37*, *38*) fail to restore significant amounts of oxygen evolution activity (*21*). In order to obtain additional information on the defect or defects caused by these mutations when reconstituted to PSII, we examined fluorescence decay kinetics in the absence or presence of DCMU to monitor possible defects on the reducing and oxidizing sides of PSII and characterized oxygen flash yields from PSII samples to determine if the S-states had been affected. The data obtained from samples to which DCMU had not been added (Figure 3, Table 1) indicate that electron transfer from Q_A^- to Q_B is unaffected by mutations to Asp157. In the presence of DCMU, where recombination between Q_A^- and the oxidizing side occurs, the fluorescence decay up to 100 ms showed very similar results for PsbO WT and Asp157 mutants, indicating that recombination between Q_A^- and $Y_Z^\bullet$ (*23*, *27*) was unaffected by Asp157 mutagenesis in PsbO. On the other hand, the slow decay component and the residual signal (Figure 4, Table 2) are increased in amplitude, but the kinetics of the slow decaying component is the same as that detected for the wild-type protein. These results indicate that the Asp157 mutations to PsbO have modified some of the properties of the oxidizing side of PSII. A more precise characterization of the defect or defects in the OEC is complicated by the fact that interpretation of the decay components in the fluorescence data assumes that all dark-adapted PSII centers are in the S_1 state. Our data indicate that this is not the case for samples reconstituted with Asp157 mutants.

Results from experiments with PSII samples reconstituted with Asp157 mutants of PsbO to examine oxygen flash yields reveal larger populations of PSII centers in the S_3 state than does a sample reconstituted with WT PsbO (Figures 5 and 6). This is consistent with previous reports documenting modifications of S-state lifetimes by either loss of PsbO-1 and replacement by the PsbO-2 protein in *Arabidopsis* (*39*, *40*) or by preparation of UW-PSII to remove PsbO, where longer S_2 and S_3 lifetimes are observed (*35*). The cause of S-state stabilization in these samples has not yet been identified. At the same time, no significant difference between PsbO WT and Asp157 mutants was detected in quantitative analyses of O_2 release kinetics, which indicates that replacement of PsbO-D157 with E, K, or N had no effect on the $S_3 \rightarrow S_0$ transition and −O−O− bond formation (Table 4). Analysis of the S-state parameters revealed that only PsbO extraction results in a sample that is susceptible to aberrant transitions (Table 3).

CONCLUSIONS

In contrast to earlier reports (*41*, *42*), the results presented in this study and in ref *21* provide evidence that PsbO-Asp157 is an important residue for optimal function of PSII. On the basis of PsbO solution structure analyses combined with activity assays, we conclude that replacement of PsbO-Asp157 with Asn, Lys, or Glu causes a defect in functional assembly of PsbO into PSII; steady-state assays of activity with these mutants revealed a defect (inefficient Cl^- retention) in PSII function (see ref *21*). The results presented here characterize the extent and nature of the defects in Asp157 mutants:

(1) Normal electron transfer between Q_A^- and Q_B is observed in UW-PSII samples reconstituted with either WT PsbO or with Asp157 mutants, which indicates that reducing side reactions of PSII are unaffected by reconstitution with the PsbO mutants.

(2) Recombination between Q_A^- and the oxidizing side of PSII is affected by the mutations, as evidenced by increased fluorescence signal amplitudes associated with the slow decay phase and residual signals in DCMU-treated samples.

(3) Oxygen flash yield measurements show the presence of a long-lived S_3 state in UW-PSII, as expected from prior investigations (*35*). Although reconstitution of UW-PSII with both WT and Asp157 mutants decreases the amount of stable S_3, reconstitution with Asp157 mutants produces a substantially larger fraction of this state than does rebinding of the WT.

(4) Oxygen release kinetics restored by reconstitution of UW-PSII with both WT and Asp157 mutant PsbO's are similar.

These results would indicate that the S_2 and S_3 states are sensitive to the defect created by Asp157 mutants in PsbO, while the $S_3 \rightarrow S_0$ transition functions normally. Although the Asp157 mutants exhibit a defect in Cl^- affinity in the OEC under steady-state illumination, the failure to overcome this defect by additions of high concentrations of Cl^- (*21*) would suggest that the modified activity of the OEC in the presence of these mutated proteins could be due to other factors as well. One possibility can perhaps be found in the recent crystal structure of cyanobacterial PSII where PsbO-D158 (homologous to D157 in spinach PsbO) is localized in proximity to the OEC active site and Cl^- is bound through a putative water molecule to the Mn_4Ca cluster at a distance of 6.5 Å, close to two proposed proton channels (*43*, *44*). Although D157 appears not to be directly involved in the proton transfer network (*21*), it is possible that assembly of a PsbO mutant lacking Asp157 creates an unfavorable environment for the function of the entire OEC. An optimizing function of Asp residues, such as sustaining structural stability, formation of hydrogen bonds, or retaining the proper orientation of surrounding molecules, has been reported for a number of other proteins (*45*−*48*).

REFERENCES

1. Nelson, N., and Yocum, C. F. (2006) Structure and function of photosystems I and II. *Annu. Rev. Plant Biol. 57*, 521–565.
2. Roose, J. L., Wegener, K. M., and Pakrasi, H. B. (2007) The extrinsic proteins of photosystem II. *Photosynth. Res. 92*, 369–387.
3. Ghanotakis, D. F., Topper, J. N., and Yocum, C. F. (1984) Structural organization of the oxidizing side of photosystem II. Exogenous reductants reduce and destroy the Mn-complex in photosystem II membranes depleted of the 17 and 23 kDa polypeptides. *Biochim. Biophys. Acta 767*, 524–531.
4. Kok, B., Forbush, B., and Mcgloin, M. (1970) Cooperation of charges in photosynthetic O_2 evolution-I. A linear four step mechanism. *Photochem. Photobiol. 11*, 457–475.
5. Hutchison, R. S., Steenhuis, J. J., Yocum, C. F., Razeghifard, M. R., and Barry, B. A. (1999) Deprotonation of the 33 kDa, extrinsic, manganese-stabilizing subunit accompanies photooxidation of manganese in photosystem II. *J. Biol. Chem. 274*, 31987–31995.
6. Hong, S. K., Pawlikowski, S. A., Vander Meulen, K. A., and Yocum, C. F. (2001) The oxidation state of the photosystem II manganese cluster influences the structure of manganese stabilizing protein. *Biochim. Biophys. Acta 1504*, 262–274.
7. Popelkova, H., Betts, S. D., Lydakis-Simantiris, N., Im, M. M., Swenson, E., and Yocum, C. F. (2006) Mutagenesis of basic residues R151 and R161 in manganese-stabilizing protein of photosystem II causes inefficient binding of chloride to the oxygen evolving complex. *Biochemistry 45*, 3107–3115.
8. Popelkova, H., Commet, A., Kuntzleman, T., and Yocum, C. F. (2008) Inorganic cofactor stabilization and retention: The unique functions of the two PsbO subunits of eukaryotic photosystem II. *Biochemistry 47*, 12953–12600.
9. Zubrzycki, I. Z., Frankel, L. K., Russo, P. S., and Bricker, T. M. (1998) Hydrodynamic studies on the manganese stabilizing protein of photosystem II. *Biochemistry 37*, 13553–13558.
10. Svensson, B., Tiede, D. M., and Barry, B. A. (2002) Small-angle X-ray scattering studies of the manganese stabilizing subunit in photosystem II. *J. Phys. Chem. B 106*, 8485–8488.
11. Uversky, V. N. (2002) What does it mean to be natively unfolded? *Eur. J. Biochem. 269*, 2–12.
12. Lydakis-Simantiris, N., Hutchison, R. S., Betts, S. D., Barry, B. A., and Yocum, C. F. (1999) Manganese stabilizing protein of photosystem II is a thermostable, natively unfolded polypeptide. *Biochemistry 38*, 404–414.
13. Popelkova, H., Im, M. M., D'Auria, J., Betts, S. D., Lydakis-Simantiris, N., and Yocum, C. F. (2002) N-terminus of the photosystem II manganese stabilizing protein: Effects of sequence elongation and truncation. *Biochemistry 41*, 2702–2711.
14. Popelkova, H., Wyman, A., and Yocum, C. F. (2003) Amino acid sequences and solution structures of manganese stabilizing protein that affect reconstitution of photosystem II activity. *Photosynth. Res. 77*, 21–34.
15. Wyman, A. J., and Yocum, C. F. (2005) Assembly and function of the photosystem II manganese stabilizing protein: Lessons from its natively unfolded behavior. *Photosynth. Res. 84*, 283–288.
16. Lydakis-Simantiris, N., Betts, S. D., and Yocum, C. F. (1999) Leucine 245 is a critical residue for folding and function of the manganese stabilizing protein of photosystem II. *Biochemistry 38*, 15528–15535.
17. Popelkova, H., Im, M. M., and Yocum, C. F. (2003) Binding of manganese stabilizing protein to photosystem II: Identification of essential N-terminal threonine residues and domains that prevent nonspecific binding. *Biochemistry 42*, 6193–6200.
18. Betts, S. D., Ross, J. R., Hall, K. U., Pichersky, E., and Yocum, C. F. (1996) Functional reconstitution of photosystem II with recombinant manganese-stabilizing protein containing mutations that remove the disulfide bridge. *Biochim. Biophys. Acta 1274*, 135–142.
19. Hutchison, R. S., Betts, S. D., Yocum, C. F., and Barry, B. A. (1998) Conformational changes in the extrinsic manganese stabilizing protein can occur upon binding to the photosystem II reaction center: An isotope editing and FT-IR study. *Biochemistry 37*, 5643–5653.
20. Wyman, A. J., Popelkova, H., and Yocum, C. F. (2008) Site-directed mutagenesis of conserved C-terminal tyrosine and tryptophan residues of PsbO, the photosystem II manganese-stabilizing protein, alters its activity and fluorescence properties. *Biochemistry 47*, 6490–6498.
21. Popelkova, H., Commet, A., and Yocum, C. F. (2009) Asp157 is required for the function of PsbO, the photosystem II manganese-stabilizing protein. *Biochemistry 48*, 11920–11928.
22. Nedbal, L., Trtilek, M., and Kaftan, D. (1999) Flash fluorescence induction: A novel method to study regulation of photosystem II. *J. Photochem. Photobiol. 48*, 154–157.
23. Reifarth, F., Christen, G., Seeliger, A. G., Dorman, P., Benning, C., and Renger, G. (1997) Modification of the water oxidizing complex in leaves of the *dgd1* mutant of *Arabidopsis thaliana* deficient in the galactolipid digalactosyldiacylglycerol. *Biochemistry 36*, 11769–11776.
24. Meunier, P. C. (1993) Oxygen evolution by photosystem II—The contributions of backward transitions to the anomalous behavior of double-hits revealed by a new analysis method. *Photosynth. Res. 36*, 111–118.
25. Shutova, T., Irrgang, K.-D., Shubin, V., Klimov, V. V., and Renger, G. (1997) Analysis of pH-induced structural changes of the isolated extrinsic 33 kilodaloton protein of photosystem II. *Biochemistry 36*, 6350–6358.
26. Bowes, J., and Crofts, A. R. (1980) Binary oscillations in the rate of reoxidation of the primary acceptor of photosystem II. *Biochim. Biophys. Acta 590*, 373–389.
27. Weiss, W., and Renger, G. (1984) Analysis of the system II reaction by UV-absorption changes in Tris-washed chloroplasts, in Advances in Photosynthesis Research (Sybesma, C., Ed.) pp 167−170, Martinus Nijhoff/Dr. W. Junk, The Hague, The Netherlands.
28. Renger, G., Gleiter, H. M., Haag, E., and Reifarth, F. (1993) Photosystem II: Thermodynamics and kinetics of electron transport from Q_A^- to Q_B and to Q_B^- and deleterious effects of copper. *Z. Naturforsch. 48c*, 234–250.
29. Roose, J. L., Frankel, L. K., and Bricker, T. M. (2010) Documentation of significant electron transport defects on the reducing side of photosystem II upon removal of the PsbP and PsbQ extrinsic proteins. *Biochemistry 49*, 36–41.
30. Crofts, A. R., and Wraight, C. A. (1983) The electrochemical domain of photosynthesis. *Biochim. Biophys. Acta 726*, 149–186.
31. Robinson, H. H., and Crofts, A. R. (1983) Kinetics of the oxidation reduction reactions of the photosystem II quinone acceptor complex and the pathway for deactivation. *FEBS Lett. 153*, 221–226.
32. Weiss, W., and Renger, G. (1984) UV spectral characterization in Tris-washed chloroplasts of the redox component-D1 which functionally connects the reaction center with the water-oxidizing enzyme system-Y in photosynthesis. *FEBS Lett. 169*, 219–223.
33. Debus, R. J. (1992) The manganese and calcium ions of photosynthetic oxygen evolution. *Biochim. Biophys. Acta 1102*, 269–352.
34. Mano, J., Takahashi, M., and Asada, K. (1987) Oxygen evolution from hydrogen peroxide in photosystem II: Flash-induced catalytic activity of water-oxidizing photosystem II membranes. *Biochemistry 26*, 2495–2501.

35. Miyao, M., Murata, N., Lavorel, J., Maison-Peteri, B., Boussac, A., and Etienne, A.-L. (1987) Effect of the 33-kDa protein on the S-state transitions in photosynthetic oxygen evolution. *Biochim. Biophys. Acta 890*, 151–159.
36. Woycechowsky, K. J., Choutko, A., Vamvaca, K., and Hilvert, D. (2008) Relative tolerance of the enzymatic molten globule and its thermostable counterpart to point mutation. *Biochemistry 47*, 13489–13496.
37. Ono, T, Zimmermann, J. L., Inoue, Y., and Rutherford, A. W. (1986) EPR evidence for the modified S-state transition in chloride-depleted photosystem II. *Biochim. Biophys. Acta 851*, 193–201.
38. Wincencjusz, H., van Gorkom, H. J., and Yocum, C. F. (1997) The photosynthetic oxygen evolution complex requires chloride for its redox state $S_2 \rightarrow S_3$ and $S_3 \rightarrow S_0$ transitions but not for $S_0 \rightarrow S_1$ or $S_1 \rightarrow S_2$ transitions. *Biochemistry 36*, 3663–3670.
39. Bricker, T. M., and Frankel, L. K. (2008) The *psbo1* mutant of *Arabidopsis* cannot efficiently use calcium in support of oxygen evolution by photosystem II. *J. Biol. Chem. 283*, 29022–2927.
40. Liu, H., Frankel, L. K., and Bricker, T. M. (2007) Functional analysis of photosystem II in a PsbO-1-deficient mutant in *Arabidopsis thaliana*. *Biochemistry 46*, 7607–7613.
41. Seidler, A., Roll, K., and Michel, H. (1992) Characterization of the 33 kDa protein of the oxygen-evolving complex of higher plants by site-directed mutagenesis, in Research in Photosynthesis (Murata, N., Ed.) Vol. *II*, pp 409−413, Kluwer Academic Publishers, Dordrecht, The Netherlands.
42. Seidler, A., Michel, H., and Rutherford, A. W. (1996) The extrinsic 33 kDa protein of photosystem II: Improved expression plasmids and progress in the mutational analysis, in Photosynthesis: From Light to Biosphere (Mathis, P., Ed.) Vol. *II*, pp 259−262, Kluwer Academic Publishers, Dordrecht, The Netherlands.
43. Loll, B., Kern, Saenger, W., Zouni, A., and Biesiadka, J. (2005) Towards complete cofactor arrangement in the 3.0 Å resolution structure of photosystem II. *Nature 438*, 1040–1044.
44. Guskov, A., Kern, J., Gabdulkhakov, A., Broser, M., Zouni, A., and Saenger, W. (2009) Cyanobacterial photosystem II at 2.9 Å resolution and the role of quinones, lipids, channels, and chloride. *Nat. Struct. Mol. Biol. 16*, 334–342.
45. Nobbs, T. J., Cortes, A., Gelpi, J. L., Holbrook, J. J., Atkinson, T., Scawen, M. D., and Nicholls, D. J. (1994) Contribution of a buried aspartate residue towards the catalytic efficiency and structural stability of *Bacillus stearothermophilus* lactate dehydrogenase. *Biochem. J. 300*, 491–499.
46. Frueauf, J. B., Ballicora, M. A., and Preiss, J. (2001) Aspartate residue 142 is important for catalysis by ADP-glucose pyrophosphorylase from *Escherichia coli*. *J. Biol. Chem. 276*, 46319–46325.
47. Kawata, M., Kinoshita, K., Takahashi, S., Ogura, K., Komoto, N., Yamanishi, M., Tobimatsu, T., and Toraya, T. (2006) Survey of catalytic residues and essential roles of glutamate-α170 and aspartate-α335 in coenzyme B_{12}-dependent diol dehydratase. *J. Biol. Chem. 281*, 18327–18334.
48. Cashin, A. L., Torrice, M. M., McMenimen, K. A., Lester, H. A., and Dougherty, D. A. (2007) Chemical-scale studies on the role of conserved aspartate in preorganizing the agonist binding site of the nicotinic acetylcholine receptor. *Biochemistry 46*, 630–639.